INTERNATIONAL JOURNAL OF CONSERVATION SCIENCE
ISSN: 2067-533X Volume 11, Special Issue 1, 2020: 223-232 www.ijcs.uaic.ro

SEM-EDS MICROANALYSIS OF ULTRATHIN GLASS AND METAL FRAGMENTS: MEASUREMENT STRATEGY BY MONTE CARLO SIMULATION IN CULTURAL HERITAGE AND ARCHAEOLOGY

Daniele MORO, Gianfranco ULIAN, Giovanni VALDRÈ*

Centro di Ricerca Interdisciplinare di Biomineralogia, Cristallografia e Biomateriali
Dipartimento di Scienze Biologiche, Geologiche e Ambientali – Università di Bologna "Alma Mater Studiorum"
Piazza di Porta San Donato 1, 40126 Bologna, Italy

Abstract

Scanning electron microscopy (SEM) combined with energy dispersive X-ray spectrometry (EDS) has a very wide range of applications in cultural heritage and archaeology, because of the capability to provide morphological analysis with high spatial resolution, combined with chemical information at the microscale. However, when the size of the materials analyzed approaches the micro- and submicrometre scale, as often found in cultural heritage and archaeology investigations, several effects related to electron and X-ray generation and transport had to be considered to avoid quantification errors. In this work, Monte Carlo simulations are presented for the study of the effects of thickness and shape on quantitative microanalysis by SEM-EDS of ultrathin glass and metal alloys fragments, as usually found in cultural heritage and archaeology. Glass fragments with different chemical composition, elongated shapes, square section and thicknesses from 0.1 to 10 µm, and micro/nanoscale gold alloy fragments were simulated in realistic experimental conditions. The simulations showed an important contribution from the fragments thickness and shape on the X-ray intensity measured by EDS, which in turn affect the quantitification procedure. The results of this study are of general meaning and application, and can be used to develop the most appropriate specific measurement strategy and avoid analytical errors and misinterpretations.

Keywords: *SEM-EDS micro-nanoanalysis; Monte Carlo simulation; Glass and metal fragments and particles*

Introduction

In a typical analytical framework in cultural heritage, the size of the available samples is very small, in order to avoid visible damages in the manufacts or for the scarse quantity and preciousness of the material. Within this picture, analytical techniques at the micrometric and nanometric scale are highly desirable for the characterization of the structure, morphology and chemistry. These advanced approaches, both at the experimental and theoretical levels [1-5], can provide both researchers and experts (e.g. restorers) invaluable results that, eventually, can be employed for the restoration and conservation of the manufacts. Scanning Electron Microscopy (SEM), together with Energy Dispersive X-ray Spectrometry (EDS) employing lithium-drifted silicon detector [Si(Li)] or silicon drift detectors (SDD), is one of such effective techniques, which allows the characterization of the morphology of the sample and correlate it to the local composition of the materials composing the specimens [1]. This approach can be

* Corresponding author: giovanni.valdre@unibo.it

successfully employed even when the sample is extremely small (micrometre and sub-micrometre scales), a common framework when it necessary to investigate glass, ceramics and lithotypes fragments and particles, or extremely thin metal and alloys sheets and bits.

In the context of such small or thin samples, it is necessary to stress that out-of-the-box analysis, i.e. using standard routine SEM/EDS configurations and arrangements (*e.g.*, energy of the primary electrons of 15-20 keV), may lead to systematic errors related to electron transport and X-ray generation and transport in both the thin materials and adjacent ones. This effect originates from the electrons elastic scattering in the finite size (mass) of the particle, that in turn is affected by the average atomic number. The X-rays intensity revealed by the detector is mainly affected by the particle size with respect to the volume of electron penetration. Thus, the standard SEM/EDS settings have to be carefully optimized when performing quantitative analyses of ultra-thin samples to avoid, or at least limit, the above-mentioned phenomena. In this sense, tailored analytical approaches must be devised by taking into account both the size and the chemical composition of the sample, a task that requires a deep knowledge on the best material-instrumental setups to advise and route the researcher to a simple, fast and significant procedure.

The aim of the present work is providing simulations of the electron transport, X-ray generation and detection in two different kind of thin materials, used as typical examples in cultural heritage and archeology. Very small glass fragments, initially modelled with a simple geometry made of elongated shapes and square section, represent the first case study. The second case study is given by thin metal sheets, resembling those found in glass mosaic tesserae, which were employed as a substrate for analysis.

Among several and fundamental computational tools for the investigation of materials at different scales [6-8], a Monte Carlo approach was here employed because it is a well-established method to model electron transport [2]. All the reported simulations were conducted considering practical experimental conditions, such as SEM-EDS arrangement, physics of the detector, and typical geometry and chemistry of the specimen. More into details, the physics governing the interaction between the electron beam and the sample (*e.g.*, electron beam energy, electron elastic/inelastic scattering, element ionization threshold levels), the setup of the chamber in the SEM-EDS instrument (*e.g.*, electron beam position on the sample, take-off and azimuthal angle of the detector), and the effects arising from the composition and thickness of the glass and metal fragments were all considered.

This kind of study is of general interest and can be of much help for the interested reader who employs SEM-EDS as an analytical technique for the investigation and quantitative characterization of very small, or thin, samples in both cultural heritage and archaeology. In fact, it is common for both researchers and restorers to deal with, just to cite some examples, paintings, surface protective treatments, surface alterations and/or contaminations, (sub-)microscopic dishomogeneity, oxidized metal surfaces. In these cases, where the sample thickness and/or lateral dimension is very small, a suitably tuned SEM-EDS approach can provide fast, accurate and consistent results whenever the dimensions of the object under investigation approaches those of the electron penetration volume.

Materials and Methods

Accurate and quantitative microanalysis of very thin samples by X-ray spectrometry requires a detailed characterization of all the effects related to the scattering of electrons inside the material, the generation and secondary fluorescence of X-rays and their absorption in various kind of materials. To this aim, the Monte Carlo simulation is an efficient methodology for modelling the transport of electrons and the generation and transport of X-rays (both characteristic and Bremmstrahlung [9-12]), also considering secondary fluorescence. This approach allows simulating the trajectories of electrons and X-rays into thin materials and the

emission to a specific EDS detector. A continuous electron energy loss (continuous slowing down approximation) and elastic scattering events are considered to model the trajectories of electrons [13]. As for the elastic scattering, the Mott cross section as described by Jablonski et al. [14], the Mott scattering cross section from Czyzewski et al. [15], and a basic screened Rutherford model [16] are employed. The continuous electron energy loss and the cross-section for ionisation are implemented with the expression of Joy-Luo [17], that is an empirical modification of the Bethe energy loss equation, and by the Bote and Salvat expression [18], respectively. The coefficients of mass absorption are those of Chantler et al. [19] and the fluorescence yields are tabulated experimental values [20].

The secondary fluorescence physics is described by the random propagation of primary X-ray emission (characteristic and Bremsstrahlung). The random direction is generated from a uniform distribution, starting from the X-ray generation point to its absorption by photoionization (taking into account the photoionization mean free path) or it leaves the material [21]. Relaxation follows the photoionization process, with the emission of characteristic X-rays from the absorbing element according to the related probabilities.

A Gaussian beam was chosen to model the electron source. Simulations of the EDS spectra were performed to investigate the effects related to the sample thickness. The acquisition of the spectra by a lithium-drifted silicon [Si(Li)] EDS detector was simulated using a function of response, mimicking the energy resolution of the detector, that was convolved with the X-rays emitted. Then, the intensity of the peaks were integrated and their trend versus the specimen thickness, the orientation and position of the detector, the position and energy of the electron beam was investigated for all the modelled materials, after background subtraction. The effects of conductive films of amorphous carbon that coats the samples were not considered in the present simulations.

Results and discussion

It is known that the SEM-EDS micro-analytical results can be affected by several effects if the sample and the electron penetration volume are very similar, as in the case of very thin materials. In conventional experimental settings (*e.g.*, beam energy in the range 10 – 30 keV), both volumes of interaction of the electron beam and X-ray generation are of the order of several μm^3 in most materials. If very thin materials are considered, the depth of penetration of the electron beam could be even more extended than the thickness of the particle, which may lead to the so-called finite size effect, namely a part of the whole electrons exits the particle or fragment before of the excitation of X-rays. The escaped electrons could then give rise to X-rays generated in the sourrounding fragments or even the underneath substrate.

In addition, the standards employed for microchemical characterizations are commonly bulk materials that can be considered of infinite size, in relation with the electron scattering, and generally with a much larger size than the unknown sample. It follows that a higher number of X-rays are generated in the reference bulk material respect to the (sub-)micrometric particle or material. Consequently, the k-ratio, *i.e.* the intensity ratio of X-rays emitted by the unknown (thin) sample to those produced by a massive sample (the standard) is further decreased due to higher X-ray intensities of the elements of the standard. It is then of utmost importance to carefully consider all these phenomena prior the analysis, to improve the quality and consistency of the experimental results.

Glass fragments

For a general explanation of the method, the simulation of the SEM/EDS analysis of glass fragments was carried out on three different kind of glasses containing silica, iron and magnesium, namely one containing sodium, one calcium and one free from any of these two elements. Glass fragments were modelled in a simple geometry consisting of elongated shape of square section, with thickness in the range 0.1 – 10 μm, placed above a bulk graphite substrate.

Table 1 reports the detailed elemental compositions in weigth % of the three considered glasses, as standards.

Table 1. Oxide contents (wt. %) in the simulated glass fragments.

Type	SiO_2	Fe_2O_3	MgO	Na_2O	CaO
1	53	35	4	8	–
2	62	2	22	–	14
3	53	40	7	–	–

For the sake of example, 2D views of the 3D simulated electron trajectories in the case of a beam of 15 keV focussed on the top of a type 3 glass fragment 2 μm thick (Fig.1a) and onto the surface of a glass fragment 200 nm thick (Fig.1b), centrally located relative to the edges, are reported in Fig.1. The electron beam (fuchsia vertical trajectory) scatters into the glass as shown by the fuchsia random trajectories. In the case of the 15 keV beam, for the 2 μm thick fragment all the electrons remain confined inside the sample, whereas for the 200 nm thick fragment the electron trajectories reach the graphite substrate (green paths) penetrating some micrometres, and possibly escaping (blue paths). In addition, some electrons exit the glass fragment laterally, both in a backscattered direction, blue trajectories, and toward the graphite, grey lines.

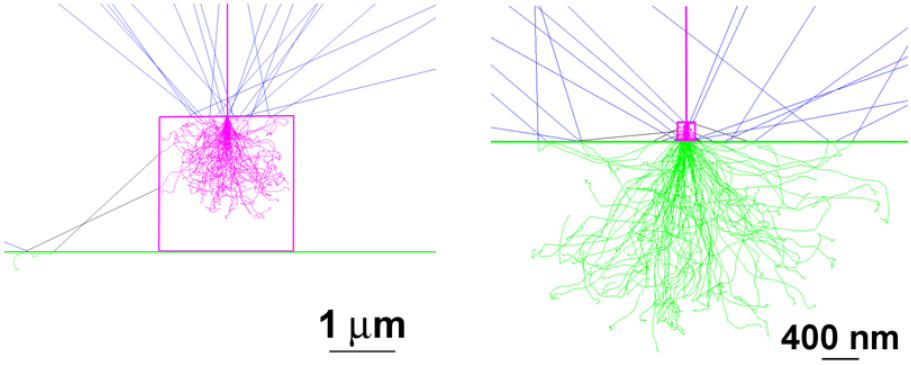

Fig. 1. Simulated trajectory of electrons, for a 15 keV energy of the primary beam, as they interact with type 3 glass fragments of square section and different size, (a) 2 μm, (b) 200 nm, positioned on a substrate of graphite.

The Monte Carlo simulation was perfromed to calculate the EDS spectra for each glass type (1, 2, 3) and thickness of the sample, versus the acceleration energy of electrons (5 keV, 15 keV and 25 keV). For the sake of an example Fig. 2 reports the integrated intensities (counts), calculated from the EDS spectra, for Si Kα and Na Kα obtained for the sodic glass (type 1), Fig. 3 shows the trends of Ca Kα, Ca Kβ and Mg Kα in the case of the calcic glass (type 2; Ca 14 wt. % and Mg 22 wt. %), whereas Fig. 4 the trends of Fe Kα, Fe Kβ, Fe L and O Kα in the case of the silica-iron-magnesium glass (type 3).

The Monte Carlo analysis shows very important results for all the glass compositions: (i) a large contribution to the variation of the calculated X-rays intensity from the thickness of the glass models, and (ii) non-linear trends for the X-ray emissions of Si, Na, Mg, Ca, Fe and O. Generally, for glass fragments with thickness approaching 10 μm the calculated intensity values were similar to those for a massive sample, independelntly of the incident beam energy (5, 15 or 25 keV).

The integrated intensities of almost all X-ray lines (Si Kα, Na Kα, Ca Kα, Ca Kβ, Mg Kα, Fe Kα, Fe Kβ, Fe L, O Kα) started reducing below a sample thickness of about 5 μm, 2 μm, and 0.5 μm, at 25 keV, 15 keV and 5 keV, respectively.

In addition, the Monte Carlo simulation showed an intensity enhancement, different for each specific X-ray emission line and electron beam energy, just before the loss of X-ray intensity, due to the small sample thickness.

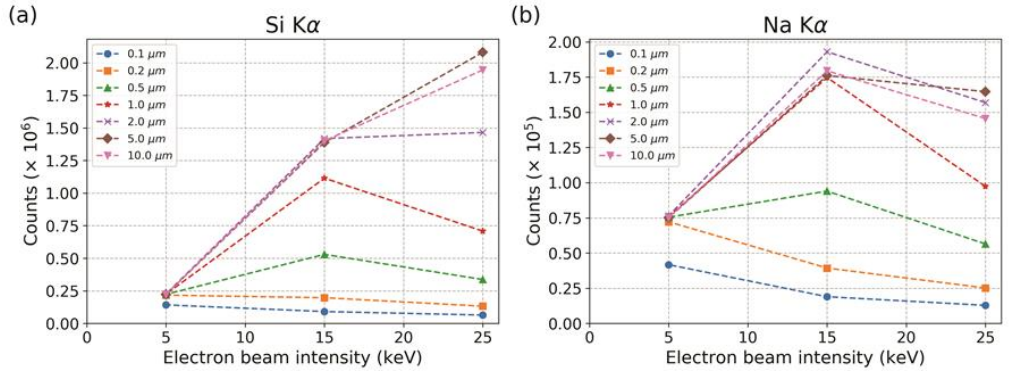

Fig. 2. SEM-EDS simulated X-ray intensity, for the sodic glass (type 1) in Table 1, as a function of electron beam acceleration energy (5, 15 and 25 keV) for different thicknesses (inset). (a) Si Kα and (b) Na Kα

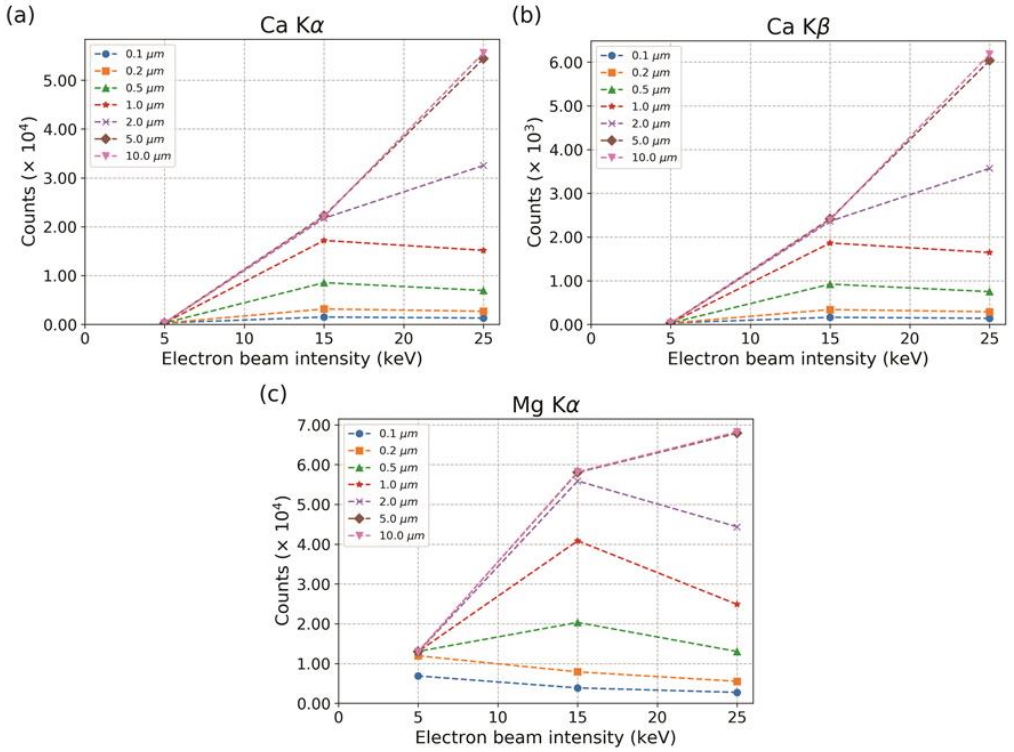

Fig. 3. SEM-EDS simulated X-ray intensity, for the calcic glass (type 2) in Table 1, as a function of electron beam acceleration energy (5, 15 and 25 keV) for different thicknesses (inset). (a) Ca Kα, (b) Ca Kα, and (c) Mg Kα

Considering the effects cited in the Introduction, related to the geometry of the glass fragments, the effect of decreased absorption (sample geometry) initially is prevalent over the finite size one (thickness), which on the contrary prevails for reduced thicknesses. In general, the magnitude of the effect of decreased X-ray absorption is higher for "soft" X-rays (Na Kα,

Fe L, O Kα), which are associated with high absorption [22]. It should be noted that Fe Kα and Fe Kβ X-ray lines cannot be excited by a beam energy of 5 keV (see Fig. 4a,b), and in the case of Ca Kα and Ca Kβ X-rays the overvoltage ratio is too low for an efficient generation (Fig. 3a,b).

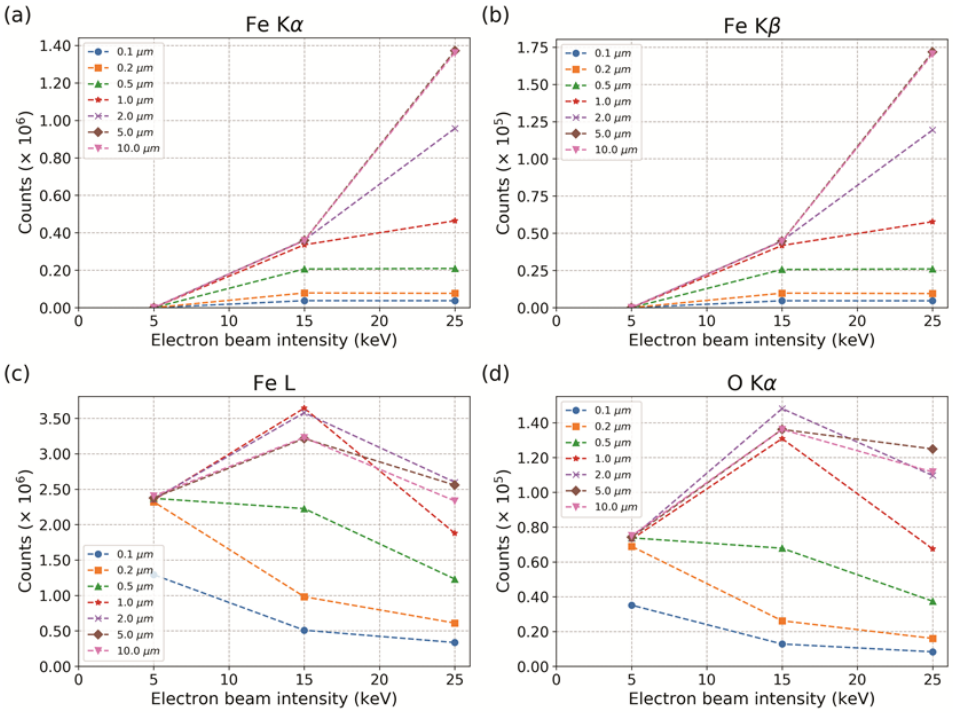

Fig. 4. SEM-EDS simulated X-ray intensity, for the silica-iron-magnesium glass (type 3) in Table 1, as a function of electron beam acceleration energy (5, 15 and 25 keV) for different thicknesses (inset). (a) Fe Kα, (b) Fe Kβ, (c) Fe L and (d) O Kα

Ultrathin metal layers

A composite sample made of a very thin metal sheet of Au-Ag-Cu alloy, sandwiched between two natron glass layers of virtually infinite thickness (mass density 2.5 g cm^{-3}), was modelled, simulating the classical geometry of gold-leaf mosaic tesserae [23]. Two gold alloy compositions were considered, whose Au-Ag-Cu content are reported in Table 2, with metal sheet thickness set to 200 nm and 1 μm, resulting in four samples with different geometry and chemistry.

The chemical quantification of the alloys were calculated by comparing the integrated intensity obtained from the simulated EDS spectra for each element in the metal sheet and calibration curves calculated for simulated massive standards. With this approach, it is possible to characterize the influence of the thickness on the micro-chemical analysis.

Table 1. Chemical composition (elements wt%) of the gold alloys simulated in ultrathin metal layer models and related mass density.

	Au	Ag	Cu	Mass density [g/cm^3]
Alloy 1	97.0	2.7	0.3	19.1
Alloy 2	93.0	6.4	0.6	18.5

An an additional effect, other than the previously cited ones, that have to be considered is related to secondary fluorescence, which is fluorescence arising if a primary X-ray (either continuum or characteristic) photoionizes an atom with the ejection of a core shell electron. Since the mean free path of energetic X-rays far exceeds the range of electrons in most materials, the secondary fluorescence can come from a material with which electrons never interacted. When the sheets are extremely thin, as the metal sheet in mosaic tesserae, and the trace elements could be distributed in the surrounding material (in this case, glass), secondary fluorescence (i.e. XRF of the glass) must be considered and properly addressed to obtain accurate chemical composition of the gold alloy.

In the case of a metal sheet with a thickness of 1 μm, a standard SEM/EDS setup, with an electron beam of 25 keV centred in the middle of the gold leaf, and the detector orientation parallel to the direction of extension of the gold sheet, gives integrated X-ray intensity comparable with the bulk sample of reference. However, a severe underestimation of about 33% for Ag and 53% for Cu was calculated for a metal sample thickness of 200 nm.

It is worth noting that the extention of the interaction volume, related to electrons transport and X-rays generation, shows a strong depence on both the energy of the primary electrons and the chemistry of materials. The scattering of electrons inside the sample affects the depth of penetration, causing a spreading of the trajectories that can extend also laterally for several micrometres. For the sake of example, the simulated X-ray emission images generated by a standard SEM/EDS setup (25 keV beam energy) in the case of a gold leaf with a thickness of 200 nm (alloy 1) is reported in Fig. 5. The tessera was modelled with the exposed metal layer (lateral portion) facing the electron beam. Fig. 5a shows an image of the simulated emission of X-rays in the case of Cu $K\alpha_1$ in the gold leaf, whereas Fig. 5b the concomitant X-ray emission in the case of Si $K\alpha_1$ for the sandwiching glasses of cartellina and support, right and left part respectively.

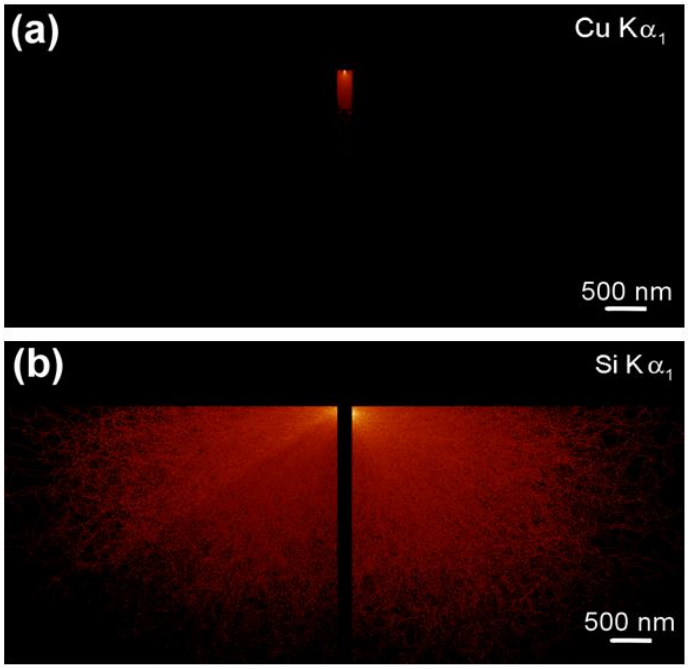

Fig. 5. Image of X-rays emission generated by a 25 keV electron beam for a gold leaf, alloy 1, with a thickness of 200 nm (a) and the sandwiching glasses (b). The colour scale, for both Cu K α_1 (a) and Si K α_1 (b), represents the intensity variation with the lighter tones meaning a higher intensity of X-rays.

The images represent a projection onto the x–z plane of the simulated three-dimensional distribution of the generation of detected X-rays. Monte Carlo simulation shows that EDS X-ray microanalysis performed with a standard SEM/EDS setup, at the modelled experimental conditions, provides indications that the volume of interaction in the metal sheet has a lateral size extended to its whole thickness (Fig. 5a). Furthermore, electron- and photo-ionization takes place in the adjacent glass layers, in the case of Si extending beyond 3 micrometers away from the metal sheet.

To confine X-ray signal generation within the ultrathin metal fragment and thus improve the analysis results, the simulations showed that, in the case of a metal sheet with thickness of 200 nm, it is necessary to reduce the energy of the primary beam to 7.5 keV. With this beam energy, the thin metal sheet behaves like a bulk sample, and SEM-EDS provides an accurate quantitative analysis of this kind of materials.

Conclusions

Several error sources which could occur in the quantitative X-ray microanalysis of ultrathin materials by SEM-EDS, such as glass fragments and metal sheets found in cultural heritage and archaeology, were here highlighted and discussed. Such effects may have heavy repercussions on other, indirect analyses of paramount importance in the context of cultural heritage and archaeology (*e.g.*, the dating of manufacts or the identification of the sources of raw material). Monte Carlo simulation proved to be very effective in addressing to the optimal instrumental setting to fully exploit the high-resolution micro-nanoanalytical potential of the SEM-EDS. Hence, it is of paramount importance to investigate and understand the limits of the methodology and identify the optimal instrumental parameters for each particular ultrathin sample and microscope, since the quantification errors may depend on several factors, such as the material thickness, composition, the specific element considered, and also the electron beam energy and other SEM-EDS experimental parameters.

References

[1] G. Giacosa, D. Moro, G. Ulian, S. Zanna, G. Valdrè, *Ceramic Recipes: Cross-correlated analytical strategy for the characterization of the Iron Age pottery from ancient Karkemish (Turkey)*, **Measurement**, **128**, 2018, pp. 180-8.

[2] D. Moro, G. Valdrè, *Effect of shape and thickness of asbestos bundles and fibres on EDS microanalysis: a Monte Carlo simulation*, **IOP Conference Series-Materials Science and Engineering**, **109**, 2016, art. 012011.

[3] G. Ulian, D. Moro, G. Valdrè, *First-principles study of structural and surface properties of (001) and (010) surfaces of hydroxylapatite and carbonated hydroxylapatite*, **Journal of Applied Crystallography**, **49**, 2016, pp.1893–1903.

[4] D. Moro, G. Valdrè, E. Mesto, F. Scordari, M. Lacalamita, G. Della Ventura, F. Bellatreccia, S. Scirè, E. Schingaro, *Hydrocarbons in phlogopite from Kasenyi kamafugitic rocks (SW Uganda): cross-correlated AFM, confocal microscopy and Raman imaging*, **Scientific Reports**, **7**, 2017, art. 40663.

[5] F. Dellisanti, A. Calafato, G.A. Pini, D. Moro, G. Ulian, G. Valdrè, *Effects of dehydration and grinding on the mechanical shear behaviour of Ca-rich montmorillonite*, **Applied Clay Science**, **152**, 2018, pp. 239-48.

[6] D. Moro, G. Ulian, G. Valdrè, *Nanoscale cross-correlated AFM, Kelvin probe, elastic modulus and quantum mechanics investigation of clay mineral surfaces: The case of chlorite*, **Applied Clay Science**, **131**, 2016, pp. 175-81.

[7] G. Ulian, D. Moro and G. Valdrè, *First principle investigation of the mechanical properties of natural layered nanocomposite: Clinochlore as a model system for heterodesmic structures*, **Composite Structures**, **202**, 2018, pp. 551-8.

[8] D. Moro, G. Ulian and G. Valdrè, *3D meso-nanostructures in cleaved and nanolithographed Mg-Al-hydroxysilicate (clinochlore): Topology, crystal-chemistry, and surface properties*, **Applied Clay Science**, **169**, 2019, pp. 74-80.

[9] S.M. Seltzer, M.J. Berger, *Bremsstrahlung spectra from electron interactions with screened atomic nuclei and orbital electrons*, **Nuclear Instruments and Methods in Physics Research Section B: Beam Interactions with Materials and Atoms**, **12(1)**, 1985, pp. 95–134.

[10] S.M. Seltzer, M.J. Berger, *Bremsstrahlung energy-spectra from electrons with kinetic-energy 1 keV-10 Gev incident on screened nuclei and orbital electrons of neutral atoms with Z = 1–100*, **Atomic Data and Nuclear Data Tables**, **35(3)**, 1986, pp. 345–418.

[11] E. Acosta, X. Llovet, F. Salvat, *Monte Carlo simulation of bremsstrahlung emission by electrons*, **Applied Physics Letters**, **80**, 2002, pp. 3228–3230.

[12] F. Salvat, J.M. Fernandez-Varea, J. Sempau, *PENELOPE-2014: A code system for Monte Carlo simulation of electron and photon transport.* Technical Report. **OECD/NEA Data Bank**, Issy-les-Moulineaux, France. 2015.

[13] N.W.M. Ritchie, *Spectrum Simulation in DTSA-II*, **Microscopy and Microanalysis**, **15**, 2009, pp. 454-68.

[14] A. Jablonski, F. Salvat, C.J. Powell, *NIST electron elastic-scattering cross-section database* (Gaithersburg, MD: National Institute of Standards and Technology), 2016.

[15] Z. Czyzewski, D.O. Maccallum, A. Romig, D.C. Joy, *Calculations of Mott Scattering Cross-Section*, **Journal of Applied Physics**, **68**, 1990, pp. 3066-72.

[16] R. Myklebust, D. Newbury, H. Yakowitz, *NBS Monte Carlo Electron Trajectory Calculation Program*, in **NBS Special Publication** (editors: K. Heinrich, H. Yakowitz, D. Newbury), **460**, 1976, p. 105, National Bureau of Standards, Washington, DC.

[17] D.C. Joy, S. Luo, *An empirical stopping power relationship for low-energy electons*, **Scanning**, **11**, 1989, pp. 176–180.

[18] D. Bote, F. Salvat, *Calculations of inner-shell ionization by electron impact with the distorted-wave and plane-wave Born approximations*, **Physical Review A**, **77**, 2008, art. 042701.

[19] C.T. Chantler, K. Olsen, R.A. Dragoset, J. Chang, A.R. Kishore, S.A. Kotochigova, D.S. Zucker, "NIST Standard Reference Database version 2.1". (Available at http://physics.nist.gov/ffast: National Institute of Standards and Technology), 2005.

[20] S.T. Perkins, D.E. Cullen, M.H. Chen, J. Rathkopf, J. Scofield, J.H. Hubbell, *Tables and graphs of atomic subshell and relaxation data derived from the LLNL Evaluated Atomic Data Library (EADL), Z = 1–100*. Technical Report. Berkley, CA: Lawrence Livermore National Laboratory, 1991.

[21] N.W.M. Ritchie, *Efficient simulation of secondary fluorescence via NIST DTSA-II Monte Carlo*, **Microscopy and Microanalysis**, **23**, 2017, pp. 618–633.

[22] J.A. Small, *The analysis of particles at low accelerating voltages (<= 10 kV) with energy daspersive x-ray spectroscopy (EDS)*, **Journal of Research of NIST**, **107**, 2002, pp. 555-66.

[23] D. Moro, G. Ulian, G. Valdrè, *Monte Carlo SEM-EDS micro- and nanoanalysis of ultrathin gold leaves in glass mosaic tesserae: Thickness effects and measurement strategy*, **Measurement**, **129**, 2018, pp. 211-7.

Received: December 5, 2019,
Accepted: February 23, 2020